Journal of King Saud University – Science 32 (2020) 2096–2102

Contents lists available at ScienceDirect

Journal of King Saud University – Science

journal homepage: www.sciencedirect.com

Original article

Numerical simulation of two-dimensional modified Helmholtz problems for anisotropic functionally graded materials

Moh. Ivan Azis [a,*], Imam Solekhudin [b], Muh. Hajarul Aswad [c], Abd. Rasyid Jalil [d]

[a] Department of Mathematics, Hasanuddin University, Indonesia
[b] Department of Mathematics, Gadjah Mada University, Indonesia
[c] Department of Mathematics, Institut Agama Islam Negeri Palopo, Indonesia
[d] Department of Marine Science, Hasanuddin University, Indonesia

ARTICLE INFO

Article history:
Received 27 March 2019
Revised 14 April 2019
Accepted 16 February 2020
Available online 22 February 2020

MSC:
65N38

Keywords:
Boundary element method
Modified Helmholtz problems
Anisotropic functionally graded media

ABSTRACT

In this paper we consider the modified Helmholtz type equation governing 2D-boundary value problems for anisotropic functionally graded materials (FGMs) with Dirichlet and Neumann boundary conditions. The persistently spatially changing diffusion and leakage factor coefficients involved in the governing equation indicate the inhomogeneity of the material under consideration. And the anisotropic diffusion coefficients indicate the material's anisotropy. Some particular examples of problems are solved numerically using a boundary element method (BEM). The results show the accuracy and consistency of the numerical solutions, the effect of the coefficient $\beta(\mathbf{x})$ values on the solutions, and the impact of the inhomogeneity and the isotropy of the materials to the solutions.

1. Introduction

Authors commonly define an FGM as an inhomogeneous material having a specific property such as thermal conductivity, hardness, toughness, ductility, corrosion resistance, etc. that changes spatially in a continuous fashion. Nowadays FGM has become an important topic, and numerous studies on FGM for a variety of applications have been reported (see e.g. Bakhadda et al., 2018; Bounouara et al., 2016; Hedayatrasa et al., 2014; Karami et al., 2017; Karami et al., 2018a; Karami et al., 2018b; Karami et al., 2018c; Karami et al., 2019a; Karami et al., 2019b and Zemri et al., 2015).

The modified Helmholtz equation appears in many kind of applications such as neutron diffusion problems (Itagaki and Brebbia, 1993), advection-diffusion problems (Solekhudin and Ang, 2012), problems governed by Laplace type equation (Chen et al., 2002), Debye-Huckel theory and the linearized Poisson–Boltzmann problems (Kropinski and Quaife, 2011), steady-state groundwater flow (Gusyev and Haitjema, 2011) and unsteady heat conduction (Guo et al., 2013). So many works which are related to the modified Helmholtz equation and focusing on finding its numerical solutions have been done, yet most of the works are limited to the case of isotropic and/or homogeneous media. The works by Igarashi and Honma (1992), Itagaki and Brebbia (1993), Singh and Tanaka (2000), Chen et al. (2002), Cheng et al. (2006), Gusyev and Haitjema (2011), Kropinski and Quaife (2011), Guo et al. (2013), Nguyen et al. (2013) and Chen et al. (2014) are among the examples.

Apparently, BEM has been successfully used for solving many types of problems of either homogeneous or functionally graded (inhomogeneous), and either isotropic or anisotropic materials. Some works using BEM for homogeneous anisotropic media of 2D diffusion-convection and Helmholtz problems (e.g. Azis et al. (2018); Azis, 2019a) have been recently reported. And for inhomogeneous anisotropic media BEM also has been used to solve elasticity, scalar elliptic, Helmholtz, diffusion-convection and diffusion-convection–reaction problems (see e.g. Azis and Clements, 2014; Azis, 2019b; Azis, 2019c; Hamzah et al., 2019; Lanafie et al., 2019; Haddade et al., 2019; Azis et al., 2019; Hamzah et al., 2019).

This paper discusses derivation of a BEM for numerically solving 2D problems governed by the modified Helmholtz type equation for anisotropic FGMs of the form

$$\frac{\partial}{\partial x_i}\left[\lambda_{ij}(x_1,x_2)\frac{\partial\phi(x_1,x_2)}{\partial x_j}\right]-\beta^2(x_1,x_2)\phi(x_1,x_2)=0 \tag{1}$$

* Corresponding author.
E-mail address: mohivanazis@yahoo.co.id (M.I. Azis).

https://doi.org/10.1016/j.jksus.2020.02.020
1018-3647/

where the coefficients λ_{ij} and β^2 depend on x_1 and x_2 and the repeated summation convention (summing from 1 to 2) is employed. In the steady-state groundwater flow, the value of $1/\beta(\mathbf{x})$ is called the "leakage factor" or "characteristic leakage length" (see Gusyev and Haitjema, 2011). Eq. (1) is relevant to modelling systems for anisotropic FGMs which are governed by the modified Helmholtz. The technique of transforming (1) to constant coefficient equations will be used for obtaining a boundary integral equation for the solution of (1). It is necessary to place some constraint on the class of coefficients λ_{ij} and β for which the solution obtained is valid.

For Eq. (1) to be an elliptic partial differential equation throughout Ω, the matrix of coefficients $[\lambda_{ij}]$ is required to be a symmetric positive definite matrix. The coefficients λ_{ij} and β are also required to be twice differentiable functions.

Throughout the paper, the analysis used is purely mathematical; to develop a BEM for obtaining the numerical solution of problems governed by Eq. (1) is the main purpose. The analysis in general applies for anisotropic media, but it is equally applicable to isotropic materials as a special case occurring when $\lambda_{11} = \lambda_{22}$ and $\lambda_{12} = 0$. Likewise, the analysis also applies especially for homogeneous materials, as a special case of FGMs, that occurs when λ_{ij} and β are constant. Therefore the main aim of this paper is to make the coverage of (1) wider as to cover the case of anisotropic FGMs as well as the special case of isotropic homogeneous materials which mostly had been worked on previously.

2. The boundary value problem

Referred to a Cartesian frame Ox_1x_2 a solution to (1) is sought which is valid in a region Ω in R^2 with boundary $\partial\Omega$ consisting of a number of piecewise continuous curves. On $\partial\Omega$ either $\phi(\mathbf{x})$ or $P(\mathbf{x})$ is specified, where

$$P(\mathbf{x}) = \lambda_{ij}(\partial\phi/\partial x_j)n_i \tag{2}$$

$\mathbf{x} = (x_1, x_2)$ and $\mathbf{n} = (n_1, n_2)$ is the normal vector pointing out on the boundary $\partial\Omega$. A boundary integral equation will be sought, from which numerical values of the dependent variables ϕ and its derivatives may be obtained for all points in Ω.

3. The boundary integral equation

The boundary integral equation is derived by transforming the variable coefficient Eq. (1) to a constant coefficient equation. We restrict the coefficients λ_{ij} and β to be of the form

$$\lambda_{ij}(\mathbf{x}) = \overline{\lambda}_{ij} g(\mathbf{x}) \tag{3}$$

$$\beta^2(\mathbf{x}) = \overline{\beta}^2 g(\mathbf{x}) \tag{4}$$

where $g(\mathbf{x})$ is a differentiable function and $\overline{\lambda}_{ij}$ and $\overline{\beta}^2$ are constant. Substitution of (3) and (4) into (1) gives

$$\overline{\lambda}_{ij}\frac{\partial}{\partial x_i}\left(g\frac{\partial\phi}{\partial x_j}\right) - \overline{\beta}^2 g\phi = 0 \tag{5}$$

Assume

$$\phi(\mathbf{x}) = g^{-1/2}(\mathbf{x})\psi(\mathbf{x}) \tag{6}$$

therefore Eq. (5) can be written as

$$\overline{\lambda}_{ij}\frac{\partial}{\partial x_i}\left[g\frac{\partial\left(g^{-1/2}\psi\right)}{\partial x_j}\right] - \overline{\beta}^2 g^{1/2}\psi = 0$$

which can be further written as

$$\overline{\lambda}_{ij}\left[\left(\frac{1}{4}g^{-3/2}\frac{\partial g}{\partial x_i}\frac{\partial g}{\partial x_j} - \frac{1}{2}g^{-1/2}\frac{\partial^2 g}{\partial x_i\partial x_j}\right)\psi + g^{1/2}\frac{\partial^2\psi}{\partial x_i\partial x_j}\right] - \overline{\beta}^2 g^{1/2}\psi = 0 \tag{7}$$

Use of the identity

$$\frac{\partial^2 g^{1/2}}{\partial x_i\partial x_j} = -\frac{1}{4}g^{-3/2}\frac{\partial g}{\partial x_i}\frac{\partial g}{\partial x_j} + \frac{1}{2}g^{-1/2}\frac{\partial^2 g}{\partial x_i\partial x_j}$$

allows Eq. (7) to be written in the form

$$g^{1/2}\overline{\lambda}_{ij}\frac{\partial^2\psi}{\partial x_i\partial x_j} - \psi\overline{\lambda}_{ij}\frac{\partial^2 g^{1/2}}{\partial x_i\partial x_j} - \overline{\beta}^2 g^{1/2}\psi = 0$$

So that if g satisfies

$$\overline{\lambda}_{ij}\frac{\partial^2 g^{1/2}}{\partial x_i\partial x_j} + k g^{1/2} = 0 \tag{8}$$

where k is a constant, then the transformation (6) brings the variable coefficients Eq. (5) into a constant coefficients equation

$$\overline{\lambda}_{ij}\frac{\partial^2\psi}{\partial x_i\partial x_j} + (k - \overline{\beta}^2)\psi = 0 \tag{9}$$

Moreover, substitution of (3) and (6) into (2) gives

$$P = -P_g\psi + P_\psi g^{1/2} \tag{10}$$

where $P_g(\mathbf{x}) = \overline{\lambda}_{ij}(\partial g^{1/2}/\partial x_j)n_i$ and $P_\psi(\mathbf{x}) = \overline{\lambda}_{ij}(\partial\psi/\partial x_j)n_i$

Three possible multi parameter function $g(\mathbf{x})$ satisfying (8) are $g(\mathbf{x}) = [A(\alpha_0 + \alpha_1 x_1 + \alpha_2 x_2)]^2$ for which $k = 0, g(\mathbf{x}) = [A\exp(\alpha_m x_m)]^2$ for which $k < 0$ and $\overline{\lambda}_{ij}\alpha_i\alpha_j = -k$, and $g(\mathbf{x}) = \{A[\cos(\alpha_m x_m) + \sin(\alpha_m x_m)]\}^2$ for which $k > 0$ and $\overline{\lambda}_{ij}\alpha_i\alpha_j = k$. When the material under consideration is a layered material consisting of several layers where each layer is a specific type of material of specific constant coefficients $\overline{\lambda}_{ij}$ and $\overline{\beta}^2$ then the discrete variation of the constant coefficients from layer to layer may certainly accommodate the determination of a continuous variation of the variable coefficients $\lambda_{ij}(\mathbf{x})$ and $\beta^2(\mathbf{x})$ by interpolation, that is to determine the parameters α_m of function $g(\mathbf{x})$.

An integral equation for (9) is

$$\eta(\mathbf{x}_0)\psi(\mathbf{x}_0) = \int_{\partial\Omega}\left[\Gamma(\mathbf{x},\mathbf{x}_0)\psi(\mathbf{x}) - \Phi(\mathbf{x},\mathbf{x}_0)P_\psi(\mathbf{x})\right]ds(\mathbf{x}) \tag{11}$$

where $\mathbf{x}_0 = (a,b), \eta = 0$ if $(a,b) \notin \Omega\cup\partial\Omega$, $\eta = 1$ if (a,b) lies inside the domain $\Omega, \eta = \frac{1}{2}$ if (a,b) is on the boundary $\partial\Omega$ given that $\partial\Omega$ has a continuously turning tangent at (a,b). The function Φ in (11) is called the fundamental solution, which is any solution of the equation $\overline{\lambda}_{ij}(\partial^2\Phi/\partial x_i\partial x_j) + (k - \overline{\beta}^2)\Phi = \delta(\mathbf{x} - \mathbf{x}_0)$ and the Γ is defined as $\Gamma(\mathbf{x},\mathbf{x}_0) = \overline{\lambda}_{ij}[\partial\Phi(\mathbf{x},\mathbf{x}_0)/\partial x_j]n_i$ where δ denotes the Dirac delta function. Following Azis (2017), for 2-D problems Φ and Γ are given by

$$\Phi(\mathbf{x},\mathbf{x}_0) = \begin{cases} \frac{K}{2\pi}\ln R & \text{if } k - \overline{\beta}^2 = 0 \\ \frac{\mathrm{i}K}{4}H_0^{(2)}(\omega R) & \text{if } k - \overline{\beta}^2 > 0 \\ \frac{-K}{2\pi}K_0(\omega R) & \text{if } k - \overline{\beta}^2 < 0 \end{cases} \tag{12}$$

$$\Gamma(\mathbf{x},\mathbf{x}_0) = \begin{cases} \frac{K}{2\pi}\frac{1}{R}\overline{\lambda}_{ij}\frac{\partial R}{\partial x_j}n_i & \text{if } k - \overline{\beta}^2 = 0 \\ \frac{-\mathrm{i}K\omega}{4}H_1^{(2)}(\omega R)\overline{\lambda}_{ij}\frac{\partial R}{\partial x_j}n_i & \text{if } k - \overline{\beta}^2 > 0 \\ \frac{K\omega}{2\pi}K_1(\omega R)\lambda_{ij}^{(0)}\frac{\partial R}{\partial x_j}n_i & \text{if } k - \overline{\beta}^2 < 0 \end{cases} \tag{13}$$

where $K = \dot{\tau}/\zeta, \omega = \sqrt{|\overline{\beta}^2/\zeta|}$, $\zeta = \left[\overline{\lambda}_{11} + 2\overline{\lambda}_{12}\dot{\tau} + \overline{\lambda}_{22}(\dot{\tau}^2 + \ddot{\tau}^2)\right]/2$, $R = \sqrt{(\dot{x}_1 - \dot{a})^2 + \left(\dot{x}_2 - \dot{b}\right)^2}, \dot{x}_1 = x_1 + \dot{\tau}x_2$, $\dot{a} = a + \dot{\tau}b, \dot{x}_2 = \ddot{\tau}x_2$ and $\dot{b} = \ddot{\tau}b$ where $\dot{\tau}$ and $\ddot{\tau}$ are respectively the real and the positive imaginary parts of the complex root τ of the quadratic $\overline{\lambda}_{11} + 2\overline{\lambda}_{12}\tau + \overline{\lambda}_{22}\tau^2 = 0$ and $H_0^{(2)}, H_1^{(2)}$ denote the Hankel function of second kind and order zero and order one respectively, K_0, K_1

denote the modified Bessel function of order zero and order one respectively and $\imath$ represents the square root of minus one. The derivatives $\partial R/\partial x_j$ necessary for the calculation of the Γ in (13) are given by $\partial R/\partial x_1 = (\dot{x}_1 - \dot{a})/R$ and $\partial R/\partial x_2 = [\dot{\tau}(\dot{x}_1 - \dot{a}) + \ddot{\tau}\left(\dot{x}_2 - \dot{b}\right)]/R$. Use of (6) and (10) in (11) yields

$$\eta(\mathbf{x}_0)g^{1/2}(\mathbf{x}_0)\phi(\mathbf{x}_0) = \int_{\partial\Omega}\left\{\left[g^{1/2}(\mathbf{x})\Gamma(\mathbf{x},\mathbf{x}_0) - P_g(\mathbf{x})\Phi(\mathbf{x},\mathbf{x}_0)\right]\phi(\mathbf{x}) - \left[g^{-1/2}(\mathbf{x})\Phi(\mathbf{x},\mathbf{x}_0)\right]P(\mathbf{x})\right\}ds(\mathbf{x}) \quad (14)$$

Eq. (14) provides a boundary integral equation which is the starting point of BEM construction for determining the numerical solutions of ϕ and its derivatives at all points of Ω.

4. Numerical examples

To illustrate the use of BEM some examples of problems governed by (1) are considered. For a simplicity, the domain Ω is taken to be a unit square for all problems (see Fig. 1). Hankel and the modified Bessel functions in (12) and (13) are approximated by their ascending series, and the integral in (14) is evaluated using Gaussian quadrature (see Abramowitz and Stegun, 1972). A number of 640 (constant) boundary elements of equal length, that is 160 elements on each side of the unit square domain, are used for the implementation of BEM.

4.1. Problems with analytical solutions

Some problems with analytical solutions will be considered. The aim is to evaluate the accuracy and efficiency of the numerical solutions. In addition to this, the impact of an increase of the coefficient $\beta(\mathbf{x})$ on the accuracy, when appropriate, will also be investigated. For all test problems considered, the boundary conditions are

ϕ given on the side AB, BC, CD
P given on the side AD

4.1.1. Example 1: anisotropic quadratically graded material

For $k = 0$ one of the possible forms of $g(\mathbf{x})$ satisfying (8) is the quadratic function $g(\mathbf{x}) = [2(1 + 2x_1 + 3x_2)]^2$ that is when a quadratically graded material is under consideration. The constant coefficient $\overline{\lambda}_{ij}$ is

$$\overline{\lambda}_{ij} = \begin{bmatrix} 1 & 1 \\ 1 & 2 \end{bmatrix}$$

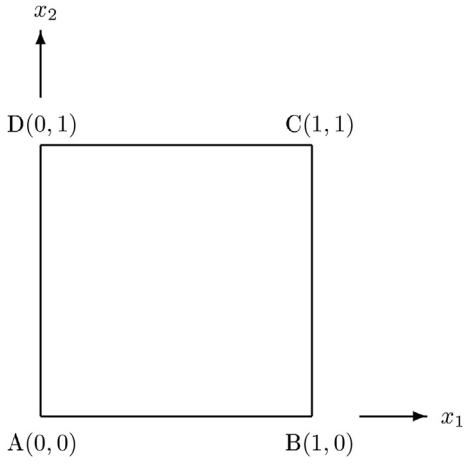

Fig. 1. The domain Ω.

We take several values of $\overline{\beta}^2$. The values of $\overline{\beta}^2$ and corresponding maximum value of wave number $\beta(\mathbf{x})$ and analytical solutions are shown in Table 1.

Table 2 shows convergence of the numerical solutions and Table 3 indicates efficiency of the BEM. Specifically, the standard BEM only needs less than a minute time to obtain the solutions $c(\mathbf{x})$ and its derivatives at 19 interior points. From this point forward, all the computation results are obtained using total number of 640 elements. Fig. 2 shows numerical ϕ absolute errors along the line $x_2 = 0.5$ for several values of $\overline{\beta}^2$. The errors are reasonably small occurring in the fourth decimal place. Fig. 2 also indicates that in general the errors increase as the value of $\overline{\beta}^2$ gets larger.

4.1.2. Example 2: anisotropic exponentially graded material

When $k < 0$ in Eq. (8), one of possible forms of $g(\mathbf{x})$ is an exponential function of the form $g(\mathbf{x}) = [2\exp(0.2x_1 + 0.3x_2)]^2$. The constant coefficients $\overline{\lambda}_{ij}$ and k are taken to be

$$\overline{\lambda}_{ij} = \begin{bmatrix} 1 & 1 \\ 1 & 2 \end{bmatrix} \quad k = -0.34$$

Table 4 shows several values of $\overline{\beta}^2$ and corresponding maximum value of wave number $\beta(\mathbf{x})$ and analytical solutions.

Fig. 3 shows numerical ϕ absolute errors along the line $x_2 = 0.5$ for several different values of $\overline{\beta}^2$. The errors occur in the fourth decimal place, even with large values of $\overline{\beta}^2$. Again, the errors increase as the value of $\overline{\beta}^2$ gets larger.

4.1.3. Example 3: anisotropic trigonometrically graded material

Another possible forms of $g(\mathbf{x})$, when $k > 0$ in Eq. (8), is a trigonometrical function $g(\mathbf{x}) = [2\{\cos(\pi x_1/4 + \pi x_2/4) + \sin(\pi x_1/4 + \pi x_2/4)\}]^2$ where $\pi = 3.1415$. Again, we take the constant coefficients $\overline{\lambda}_{ij}$ and k

$$\overline{\lambda}_{ij} = \begin{bmatrix} 1 & 1 \\ 1 & 2 \end{bmatrix} \quad k = 5\pi^2/16$$

We intend to set the value of the coefficient $(k - \overline{\beta}^2)$ in (9) to be negative, zero and positive, so as to consider three different types of Eq. (9). Therefore we choose $\overline{\beta}^2 = 9\pi^2/16, 5\pi^2/16, \pi^2/16$ thus $k - \overline{\beta}^2 = -\pi^2/4, 0, \pi^2/4$. Table 5 shows the values of $\overline{\beta}^2$ and corresponding analytical solutions.

Fig. 4 shows numerical ϕ absolute errors along the line $x_2 = 0.5$ for three different values of $\overline{\beta}^2$. As for each $\overline{\beta}^2$ represents a different type of Eq. (9), it is inappropriate to make a conclusion regarding the effect of $\overline{\beta}^2$ values change on the errors.

4.2. Problems without any simple analytical solutions

Two problems will be considered. The boundary conditions are

$P = 0$ on the side AB
$\phi = 0$ on the side BC
$P = 0$ on the side CD
$P = 100$ on the side AD

Table 1
The values of $\overline{\beta}^2$ and corresponding maximum $\beta(\mathbf{x})$ and analytical solutions for Example 1.

$\overline{\beta}^2$	max $\beta(\mathbf{x})$	Analytical solution $\phi(\mathbf{x})$
0.3125	6.71	$\frac{\exp[0.25(x_1+x_2)]}{2(1+2x_1+3x_2)}$
1.25	13.41	$\frac{\exp[0.5(x_1+x_2)]}{2(1+2x_1+3x_2)}$
5	26.83	$\frac{\exp(x_1+x_2)}{2(1+2x_1+3x_2)}$
20	53.66	$\frac{\exp[2(x_1+x_2)]}{2(1+2x_1+3x_2)}$

Table 2
Convergence of solutions for Example 1 of the case $\overline{\beta}^2 = 20$.

Point	160 elements	320 elements	640 elements	Analytical
(0.1,0.5)	0.6154	0.6153	0.6150	0.6148
(0.3,0.5)	0.7993	0.7993	0.7991	0.7989
(0.5,0.5)	1.0561	1.0560	1.0558	1.0556
(0.7,0.5)	1.4140	1.4137	1.4135	1.4132
(0.9,0.5)	1.9131	1.9129	1.9125	1.9122

Table 3
CPU computation time (in seconds) for Example 1 of the case $\overline{\beta}^2 = 20$.

160 elements	320 elements	640 elements
4.59375	16.03125	59.65625

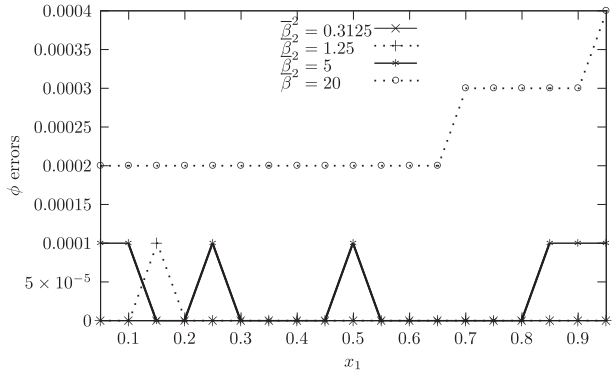

Fig. 2. Numerical ϕ absolute errors along the line $x_2 = 0.5$ for Example 1.

Table 4
The values of $\overline{\beta}^2$ and corresponding maximum $\beta(\mathbf{x})$ and analytical solutions for Example 2.

$\overline{\beta}^2$	max $\beta(\mathbf{x})$	Analytical solution $\phi(\mathbf{x})$
0	0	0.5
0.31	1.84	$0.5\exp(0.1x_1 + 0.1x_2)$
0.91	3.14	$0.5\exp(0.3x_1 + 0.2x_2)$
4.66	7.12	$0.5\exp(0.8x + 0.7x_2)$
19.66	131.59	$0.5\exp(1.8x_1 + 1.7x_2)$

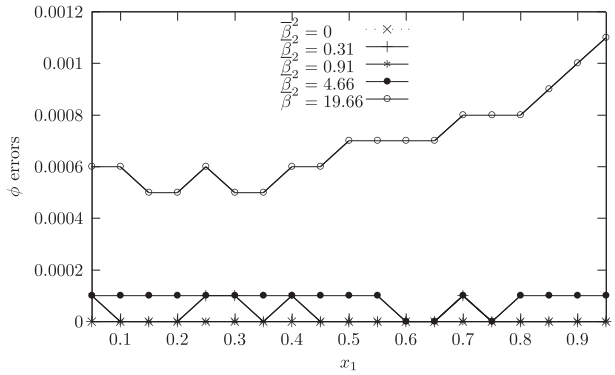

Fig. 3. Numerical ϕ absolute errors along the line $x_2 = 0.5$ for Example 2.

Table 5
The values of $\overline{\beta}^2$ and corresponding analytical solutions for Example 3.

$\overline{\beta}^2$	Analytical solution $\phi(\mathbf{x})$
$\frac{9}{16}\pi^2$	$\frac{0.5\exp\left[\frac{\pi}{\sqrt{20}}(x_1+x_2)\right]}{\cos\left[\frac{\pi}{4}(x_1+x_2)\right]+\sin\left[\frac{\pi}{4}(x_1+x_2)\right]}$
$\frac{5}{16}\pi^2$	$\frac{0.5(1+x_1+x_2)}{\cos\left[\frac{\pi}{4}(x_1+x_2)\right]+\sin\left[\frac{\pi}{4}(x_1+x_2)\right]}$
$\frac{1}{16}\pi^2$	$\frac{\cos\left[\frac{\pi}{\sqrt{20}}(x_1+x_2)\right]+\sin\left[\frac{\pi}{\sqrt{20}}(x_1+x_2)\right]}{2\left\{\cos\left[\frac{\pi}{4}(x_1+x_2)\right]+\sin\left[\frac{\pi}{4}(x_1+x_2)\right]\right\}}$

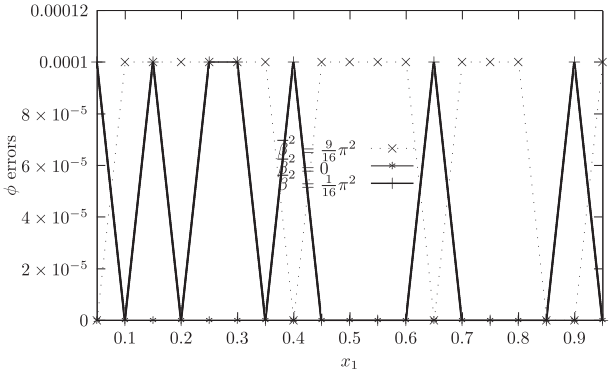

Fig. 4. Numerical ϕ absolute errors along the line $x_2 = 0.5$ for Example 3.

4.2.1. Example 4

Now, the purpose is to show coherence between the flow vector $\left(\frac{\partial\phi}{\partial x_1}, \frac{\partial\phi}{\partial x_2}\right)$ and the scattering ϕ solutions inside the domain, and the impact of the inhomogeneity and the anisotropy of the material. The variable coefficients $\lambda_{ij}(\mathbf{x})$ and $\beta^2(\mathbf{x})$ for the governing Eq. (1) are

$$\begin{aligned} \lambda_{ij}(\mathbf{x}) &= \overline{\lambda}_{ij} g(\mathbf{x}) \\ \beta^2(\mathbf{x}) &= \overline{\beta}^2 g(\mathbf{x}) \\ g(\mathbf{x}) &= [2(\alpha_0 + \alpha_1 x_1 + \alpha_2 x_2)]^2 \\ \overline{\beta}^2 &= 20 \end{aligned}$$

And we consider two cases regarding the anisotropy $(\overline{\lambda}_{ij})$ and inhomogeneity $(g(\mathbf{x}))$ of the material as shown in Table 6.

Figs. 5 and 6 show a coherence between the flow vector and scattering ϕ solutions. This verifies that the developed FORTRAN code computes the flow vector correctly.

Table 6
Two cases regarding the anisotropy $(\overline{\lambda}_{ij})$ and inhomogeneity $(g(\mathbf{x}))$ for Example 4.

Material	$\overline{\lambda}_{ij}$	$g(\mathbf{x})$
Isotropic homogeneous	$\begin{bmatrix} 1 & 0 \\ 0 & 1 \end{bmatrix}$	4
Anisotropic inhomogeneous	$\begin{bmatrix} 1 & 1 \\ 1 & 2 \end{bmatrix}$	$[2(1 + 2x_1 + 3x_2)]^2$

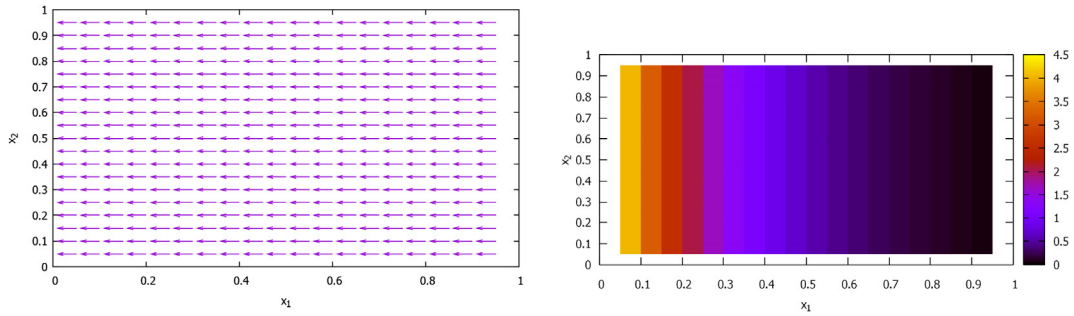

Fig. 5. Flow and scattering solutions for Example 4 of the isotropic homogeneous material.

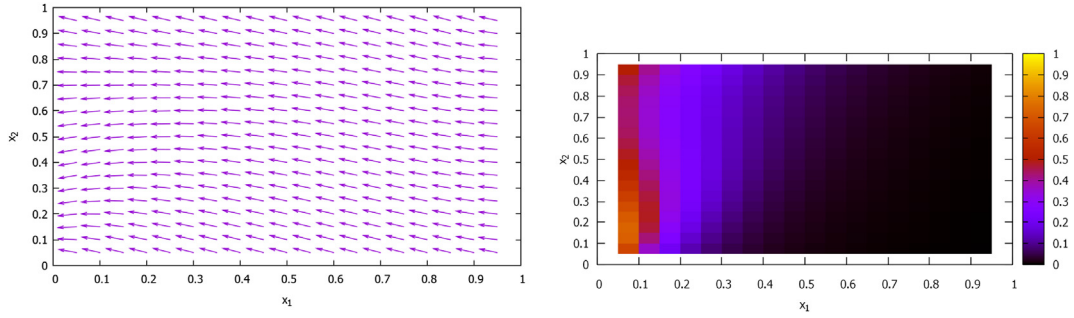

Fig. 6. Flow and scattering solutions for Example 4 of the anisotropic inhomogeneous material.

Table 7
The values of constant matrix $\overline{\lambda}_{ij}$ and the parameters α_m for Example 5.

Material	$\overline{\lambda}_{ij}$	$g(\mathbf{x})$
Isotropic homogeneous	$\begin{bmatrix}1 & 0\\ 0 & 1\end{bmatrix}$	$A=2, \alpha_0=1, \alpha_1=0, \alpha_2=0$
Isotropic inhomogeneous	$\begin{bmatrix}1 & 0\\ 0 & 1\end{bmatrix}$	$A=2, \alpha_0=1, \alpha_1=\frac{7\pi}{16}, \alpha_2=\frac{7\pi}{16}$
Anisotropic homogeneous	$\begin{bmatrix}1 & 1\\ 1 & 2\end{bmatrix}$	$A=2, \alpha_0=1, \alpha_1=0, \alpha_2=0$
Anisotropic inhomogeneous	$\begin{bmatrix}1 & 1\\ 1 & 2\end{bmatrix}$	$A=2, \alpha_0=1, \alpha_1=\frac{7\pi}{16}, \alpha_2=\frac{7\pi}{16}$

4.2.2. Example 5

The aim is to see comparison of solutions for quadratically, exponentially and trigonometrically graded materials by keeping the parameters A, α_m of the function $g(\mathbf{x})$, and the constant coefficients $\overline{\lambda}_{ij}, \overline{\beta}^2$ the same for all types of graded materials. Three types of material's gradation and their forms of function $g(\mathbf{x})$ are

$$\begin{aligned}
\text{quadratical} \quad & g(\mathbf{x}) = [A(\alpha_0 + \alpha_m x_m)]^2,\ k = 0\\
\text{exponential} \quad & g(\mathbf{x}) = [A\exp(\alpha_m x_m)]^2,\ k = -\overline{\lambda}_{ij}\alpha_i\alpha_j\\
\text{trigonometrical} \quad & g(\mathbf{x}) = [A\{\cos(\alpha_m x_m) + \sin(\alpha_m x_m)\}]^2,\ k = \overline{\lambda}_{ij}\alpha_i\alpha_j
\end{aligned}$$

The parameter $\overline{\beta}^2$ chosen is $\overline{\beta}^2 = 20$ and the values of constant matrix $\overline{\lambda}_{ij}$ and the parameters α_m associated with the anisotropy and inhomogeneity of the material are shown in Table 7.

Table 8 shows a comparison of ϕ solutions inside the unit square domain for each combination of isotropy and homogeneity, and each type of types of material's gradation. The results in Table 8 may be described as follows:

- for each type of material, the impact of the anisotropy and inhomogeneity on the solutions is evident. This suggests that it is important to take into account the anisotropy as well as the inhomogeneity in application.
- when the material is homogeneous (ie. $\alpha_1 = 0, \alpha_2 = 0$ so that $k = 0$), either the material is isotropic or anisotropic, all the three types of material give identical solutions since the problems are identical.
- contrarily, when the material is inhomogeneous (ie. $\alpha_1 = \frac{7\pi}{16}, \alpha_2 = \frac{7\pi}{16}$) the scattering solutions of the three types of material's gradation are different. This is due to that the problems are not identical (the value k in Eqs. (8) and (9) is different) for each type of material's gradation.

5. Conclusion

It is possible to find numerical solutions of problems governed by an equation of variable coefficients such as the modified Helmholtz type Eq. (1) by using a standard BEM. Being adopted in this work, transformation of the variable coefficient equation into a constant coefficient equation is among way to derive a boundary integral equation. A BEM may then be constructed from the boundary integral equation. The standard BEM provides an ease of implementation, timeless computation and accurate solutions.

Modeling physical application for an anisotropic FGM always involves a variable coefficients governing equation such as (1). In this paper, quadratically, exponentially and trigonometrically graded materials are considered as the FGMs.

In addition to its accuracy, the BEM has also been working properly. This is indicated by the consistency between the flow vectors and scattering solutions. Moreover, it is also observed that the

Table 8
Comparison of ϕ solutions for Example 5.

Quadratic	Exponential	Trigonometrical
Isotropic homogeneous		
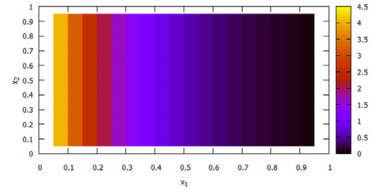	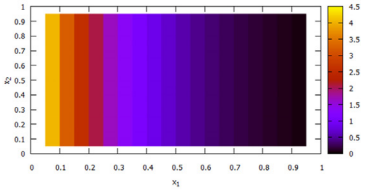	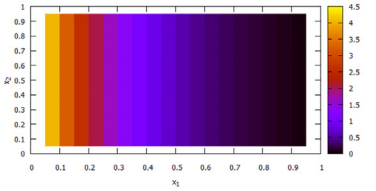
Isotropic inhomogeneous		
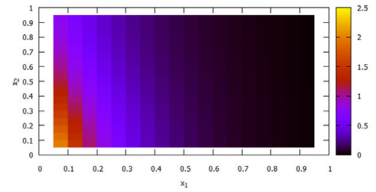	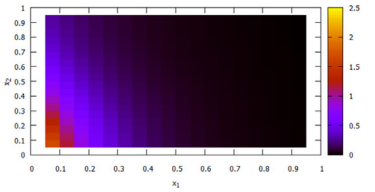	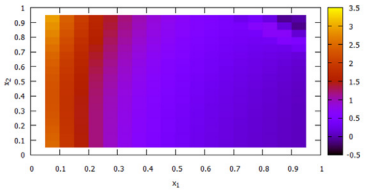
Anisotropic homogeneous		
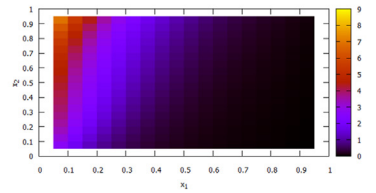	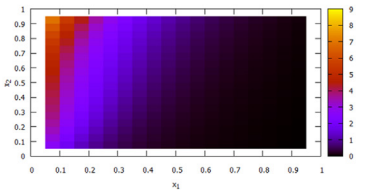	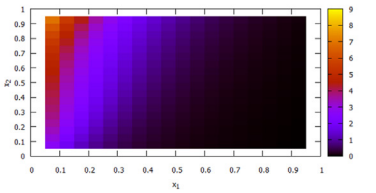
Anisotropic inhomogeneous		
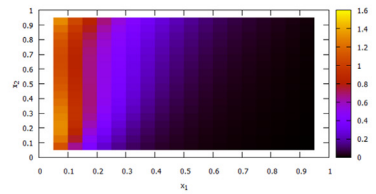	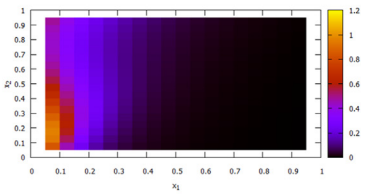	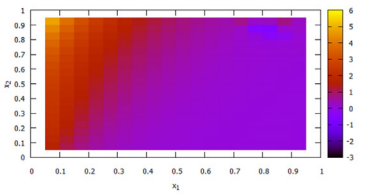

anisotropy and inhomogeneity of the material effect the results. This suggests both anisotropy and inhomogeneity should be taken into account in applications.

Acknowledgements

This work was supported by the Hasanuddin University, the Ministry of Education and Culture, and the Ministry of Finance of the Republic of Indonesia.

References

Abramowitz, M., Stegun, I.A., 1972. Handbook of Mathematical Functions: With Formulas, Graphs and Mathematical Tables. Dover Publications, Washington.
Azis, M.I., 2017. Fundamental solutions to two types of 2D boundary value problems of anisotropic materials. Far East J. Math. Sci. 101 (11), 2405–2420.
Azis, M.I., 2019a. Numerical solutions for the Helmholtz boundary value problems of anisotropic homogeneous media. J. Comput. Phys. 381, 42–51.
Azis, M.I., 2019b. Standard-BEM solutions to two types of anisotropic-diffusion convection reaction equations with variable coefficients. Eng. Anal. Boundary Elem. 105, 87–93.
Azis, M.I., 2019c. Numerical solutions to a class of scalar elliptic BVPs for anisotropic exponentially graded media. J. Phys: Conf. Ser. 1218, 012001.
Azis, M.I., Clements, D.L., 2014. A boundary element method for transient heat conduction problem of non homogeneous anisotropic materials. Far East J. Math. Sci. 89 (1), 51–67.
Azis, M.I., Kasbawati, Haddade, A., Thamrin, S.A., 2018. On some examples of pollutant transport problems solved numerically using the boundary element method. J. Phys: Conf. Ser. 979 (1).
Azis, M.I., Syam, R., Hamzah, S., 2019. BEM solutions to BVPs governed by the anisotropic modified Helmholtz equation for quadratically graded media. IOP Conf. Ser.: Earth Environ. Sci. 279, 012010.
Bakhadda, B., Bouiadjra, M.B., Bourada, F., Bousahla, A.A., Tounsi, A., Mahmoud, S.R., 2018. Dynamic and bending analysis of carbon nanotube-reinforced composite plates with elastic foundation. Wind Struct., Int. J. 27 (5), 311–324.
Bounouara, F., Benrahou, K.H., Belkorissat, I., Tounsi, A., 2016. A nonlocal zeroth-order shear deformation theory for free vibration of functionally graded nanoscale plates resting on elastic foundation. Steel Compos. Struct. 20 (2), 227–249.
Chen, K.H., Chen, J.T., Chou, C.R., Yueh, C.Y., 2002. Dual boundary element analysis of oblique incident wave passing a thin submerged breakwater. Eng. Anal. Boundary Elem. 26, 917–928.

Chen, W., Zhang, J.-Y., Fu, Z.-J., 2014. Singular boundary method for modified Helmholtz equations. Eng. Anal. Boundary Elem. 44, 112–119.
Cheng, H., Huang, J., Leiterman, T.J., 2006. An adaptive fast solver for the modified Helmholtz equation in two dimensions. J. Comput. Phys. 211, 616–637.
Guo, S., Zhang, J., Li, G., Zhou, F., 2013. Three-dimensional transient heat conduction analysis by Laplace transformation and multiple reciprocity boundary face method. Eng. Anal. Boundary Elem. 37, 15–22.
Gusyev, M.A., Haitjema, H.M., 2011. An exact solution for a constant-strength line-sink satisfying the modified Helmholtz equation for groundwater flow. Adv. Water Resour. 34, 519–525.
Haddade, A., Azis, M.I., Djafar, Z., Jabir, St.N., Nurwahyu, B., 2019. Numerical solutions to a class of scalar elliptic BVPs for anisotropic quadratically graded media. IOP Conf. Ser.: Earth Environ. Sci. 279, 012007.
Hamzah, S., Azis, M.I., Haddade, A., Syamsuddin, E., 2019. On some examples of BEM solution to elasticity problems of isotropic functionally graded materials. IOP Conf. Ser.: Mater. Sci. Eng. 619, 012018.
Hamzah, S., Azis, M.I., Haddade, A., Amir, A.K., 2019. Numerical solutions to anisotropic BVPs for quadratically graded media governed by a Helmholtz equation. IOP Conf. Ser.: Mater. Sci. Eng. 619, 012060.
Hedayatrasa, S., Bui, T.Q., Zhang, C., Lim, C.W., 2014. Numerical modeling of wave propagation in functionally graded materials using time-domain spectral Chebyshev elements. J. Comput. Phys. 258, 381–404.
Igarashi, H., Honma, T., 1992. On axially and helically symmetric fundamental solutions to modified Helmholtz-type equations. Appl. Math. Model. 16, 314–319.
Itagaki, M., Brebbia, C.A., 1993. Multiple reciprocity boundary element formulation for one-group fission neutron source iteration problems. Eng. Anal. Boundary Elem. 11, 39–45.
Karami, B., Janghorban, M., Tounsi, A., 2017. Effects of triaxial magnetic field on the anisotropic nanoplates. Steel Compos. Struct. 25 (3), 361–374.
Karami, B., Janghorban, M., Tounsi, A., 2018a. Nonlocal strain gradient 3D elasticity theory for anisotropic spherical nanoparticles. Steel Compos. Struct. 27 (2), 201–216.
Karami, B., Janghorban, M., Tounsi, A., 2018b. Variational approach for wave dispersion in anisotropic doubly-curved nanoshells based on a new nonlocal strain gradient higher order shell theory. Thin-Walled Struct. 129, 251–264.
Karami, B., Janghorban, M., Tounsi, A., 2018c. Galerkin's approach for buckling analysis of functionally graded anisotropic nanoplates/different boundary conditions. Eng. Comput. In press.
Karami, B., Janghorban, M., Tounsi, A., 2019a. On exact wave propagation analysis of triclinic material using three-dimensional bi-Helmholtz gradient plate model. Struct. Eng. Mech. 69 (5), 487–497.
Karami, B., Shahsavari, D., Janghorban, M., Tounsi, A., 2019b. Resonance behavior of functionally graded polymer composite nanoplates reinforced with graphene nanoplatelets. Int. J. Mech. Sci. 156, 94–105.
Kropinski, M.C.A., Quaife, B.D., 2011. Fast integral equation methods for the modified Helmholtz equation. J. Comput. Phys. 230, 425–434.
Lanafie, N., Azis, M.I., Haddade, A., Fahruddin, 2019. Numerical solutions to BVPs governed by the anisotropic modified Helmholtz equation for trigonometrically graded media. IOP Conf. Ser.: Mater. Sci. Eng. 619, 012058.
Nguyen, H.T., Tran, Q.V., Nguyen, V.T., 2013. Some remarks on a modified Helmholtz equation with inhomogeneous source. Appl. Math. Model. 37, 793–814.
Singh, K.M., Tanaka, M., 2000. On exponential variable transformation based boundary element formulation for advection–diffusion problems. Eng. Anal. Boundary Elem. 24, 225–235.
Solekhudin, I., Ang, K.-C., 2012. A DRBEM with a predictor-corrector scheme for steady infiltration from periodic channels with root-water uptake. Eng. Anal. Boundary Elem. 36, 1199–1204.
Zemri, A., Houari, M.S.A., Bousahla, A.A., Tounsi, A., 2015. A mechanical response of functionally graded nanoscale beam: an assessment of a refined nonlocal shear deformation theory beam theory. Struct. Eng. Mech. 54 (4), 693–710.